TELKOMNIKA Indonesian Journal of Electrical Engineering
Vol.12, No.3, March 2014, pp. 1741 ~ 1750
DOI: http://dx.doi.org/10.11591/telkomnika.v12i3.4478

Moisture Transfer Models and Drying Characteristics of MSW Containing High Moisture

Chen Shu*[1, 2], Ma Xiao-Qian[1], Liang Zeng-Ying[3]
[1]School of Electric Power, South China University of Technology, China
[2]College of Electromechanical Engineering, Zhongkai University of Agriculture and Technology, China
[3]ShenZhen Energy Environment Engineering CO.LTD, China
*Corresponding author, e-mail: weilachen@163.com

Abstract

In the present study, the effect of high moisture content on drying characteristics of watery municipal solid waste (MSW) material, such as kitchen garbage carrot peel and pomelo peel were investigated. In order to clarify the moisture transfer characteristics, selected published mathematical drying models, were fitted to experimental data using non-linear regression analysis techniques. The experimental data used to fit the drying models of samples were conducted in a thermogravimetric furnace. Weight reduction during drying was measured with a microbalance in the temperature range of 80-140℃. In addition, the variations of moisture content and drying rate at different temperature were considered. The results show that with increased in drying temperature the drying time decreased and the maximum drying rate increased at the beginning of drying process. The effective diffusivity ranged from 1.49×10^{-9} to 1.25×10^{-8}m2/s with Fick's diffusion equation. The activation energy value of 17.12kJ/mol and 37.48kJ/mol was determined through Arrhenius equation. Six different drying models were fitted to the experimental data as comparing the correlation coefficient and chi-squared value. The Modified Page model and Weibull distribution model were found to be the most adequate models in describing the drying of high moisture MSW. Correlations expressing the two models constants are reported.

***Keywords**: high moisture MSW drying, drying curves, drying models, drying kinetics*

1. Introduction

The safe disposal of municipal solid waste has now become an urgent environmental problem as the traditional method use of landfilling is rapidly declining with the depletion of available land resources and appearance of pollution environment in China. The garbage power generation has both good social and economic benefits. Incineration is widely accepted as an alternate means to dispose solid waste as developing countries recognize the environmentally friendly advantages of this technology by comparision with other methods [1, 2]. An efficient incinerator is not only assessed by the amount of heat recovery but also by the levels of emissions and quality of the ash it produces.

The solid fuel consists of four components: moisture, volatile matter, fixed carbon and ash. The incineration process of solid wastes is divided into four successive stages: evaporation of moisture from the solids; volatile release/char formation; burning of the hydrocarbon volatiles in the gaseous space; and the combustion of char particles. The moisture content in the waste begins to be reduced at the bottom of the bed as hot air (373K) from the grate drives it out, radiation from high temperature flue gas and convection from the hot furnace gases. This is followed by a process in which volatile material evolves from the fuel, ignites, and burns. Finally, the fixed carbon in the devolatilized waste particles ignites and burns.

It is well known the fact that change in moisture content has an important impact on the burning rate of fuel and high levels of moisture cause difficulty in ignition. More importantly, high moisture levels affect the combustion efficiency (unburned char in exit ash), emission of harmful gases (CO, VOC, hydrocarbon, NOX, dioxin etc.), heavy metal partition between solid and gas phases and flame stability [3].

The early works about drying process mainly concentrate on research in food and the crops [4-7], and the ambient temperature for drying is generally lower than 100℃. The purpose of drying is to reduce the moisture content for preservation and easy for storage. However,

Received August 18, 2013; Revised September 28, 2013; Accepted October 7, 2013

municipal solid waste is a mixture consisting of multi-components and prone to affect substantial variations in the fuel properties, particularly in the moisture content due to weather and seasonal change, and also by regions. And each composition has its own physical characteristics and chemical properties. The purpose of waste drying is to prepare for future burning, and the dry ambient temperature is higher than 100℃.

Generally, garbage from a home kitchen contains higher water content compared with other municipal waste such as wood, paper and plastic. Wet garbage is incombustible material, and it is difficult to recover the thermal energy. Thus, it is very important to determine the effect of water content on drying characteristics of wet waste material. In order to obtain the fundamental data for drying of wet material, carrot peel and pomelo peel were selected as materials to be tested in the dry ambient temperature range of 80-140℃. The behaviors during drying were investigated. Weight reduction and drying time for the drying of samples containing water were measured. The relations between moisture rate and drying time, the drying rate and moisture rate during the drying process were analyzed.

Mathematical modeling of MSW drying is important for optimization of operating parameters and performance improvements of the drying systems. The main advantage of models in drying simulations is easy to apply. Several researchers have evaluated different mathematical models for high moisture MSW. Chen and Wu evaluated mathematical models for drying of rough rice with high moisture ratio and found two-term exponential model was the best fit drying models [8]. M.C.Garau et al. investigated drying kinetics modeling and functional properties of orange skin and indicated that diffusional model was the best fit drying models [9]. G. Ruíz Díaz et al. adopted Peleg's and Weibull's equations to simulate the drying of orange slices [10]. Three different drying models were fitted to the experimental data of moisture ration for potato drying and Page model was found as the best fit [11]. E.Akpinar et al. suggested the diffusion model for drying behaviour of potato slices [12]. Ebru Kavak Akpinar presented that semi-theoretical Midilli-Kucuk model was the best mathematical modeling of thin layer drying of potato, apple and pumpkin slices in a convective cyclone dryer [13].

In the present study, experimental data for carrot peel and pomelo peel are used in order to study the influence of temperature on MSW drying curves, and evaluate alternate empirical or simple phenomenological models reported in literature to simulate the drying curves of high moisture MSW, and propose a simple model to accurately simulate the drying kinetics of MSW at different drying air temperatures. These results will help to further understanding of the drying characteristics of high moisture municipal solid waste and improve the efficiency of municipal incinerators.

2. Materials and Methods

2.1. Sample Material

In the experiment, carrot peel and pomelo peel were selected as the sample material in order to investigate the effect of water moisture on drying. Carrot peel and pomelo peel are unwanted parts from the kind of popular vegetable and fruit in south China, and they are readily available. The drying ambient temperature is in the range of 80-140℃. The carrot test pieces had volume of 20mm×5mm×2mm; the pomelo test pieces had volume of 8mm×8mm×8mm. The samples were evenly spread on the drying pan and completely covering the base.

2.2. Experimental Facility

The schematic diagram of experimental apparatus is shown in Figure 1. A cubic-type electric furnace had 450mm length, 350mm width and 450mm height. A small test piece was placed on the square plat of the supporting stage. The change in weight of the test pieces were measured using an electric microbalance set below the furnace bench. The output signal from the electric microbalance was treated using a computer through visual basic programming, and the weight loss during drying was recorded. In order to measure the temperature in the electric furnace during drying, a K-type thermocouple was set at the position of double height above the test piece. The output from the thermocouple was displayed on the panel of the electric furnace.

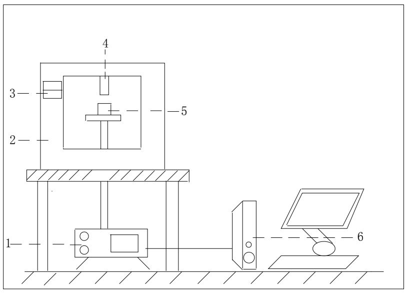

1. Electronic Balance 2. Air Drying Oven 3.thermostat 4.Thermocouple 5.sample 6.computer

Figure 1. Schematic Diagram of Experimental Apparatus

2.3. Mathematical Modeling of the Drying Curves

Depending on the applied equations, drying models can be classified as theoretical, semi-empirical and empirical models [14]. The major difference between these groups is that the theoretical models suggest that the moisture transport is controlled mainly by internal resistance mechanisms, while the other two consider only external resistance [15]. The semi-theoretical models are derived directly from the general solution of Fick's law by simplification. The empirical models are derived from statistical relations and they directly correlate moisture content with time, having no physical connection with the drying process itself. These types of models (empirical and semi-empirical) are valid in the specific ranges of temperature, air velocity and humidity for which they are developed.

The transport of water shows two main periods during waste dehydration process: the constant rate period and falling rate period. The falling rate period is the most important in a dehydration process and the mechanisms in this period are more complex. This is controlled by the liquid diffusion mechanism and can be described by the Fick's second law, when radial diffusion is considered [16].

Knowledge of drying kinetics is important in the design, simulation and optimization of waste drying processes. Drying curves are usually modeled by defining drying rate constants based on first order kinetics. The basic model is known as the exponential Lewis model (Eq. (1)), assuming that the moisture content depends only on time [17].

$$MR = \frac{M(t) - M_{eq}}{M_0 - M_{eq}} = \exp(-kt) \tag{1}$$

Where, MR is the moisture ratio, as the dimensionless form of moisture content, M_0 is the initial moisture content per dry unit waste, M_{eq} is the equilibrium moisture content per dry unit waste (g water/g dry matter), M_t is the real-time moisture content per dry unit waste (g water/g dry matter), k is drying constant and t is time (s).

The moisture ratio determines the unaccomplished moisture change, defined as the ratio of the free water still to be removed, as time t over the initial total free water.

Sharaf-Eldeen, Blaisdell, and Hamdy presented the two-term exponential model [18] (Equation (2)):

$$MR = \frac{M(t) - M_{eq}}{M_0 - M_{eq}} = a\exp(-k_0 t) + b\exp(-k_1 t) \tag{2}$$

Where a, b, k_0, k_1 are proportionality constants.

Based on the classical solution of the liquid diffusion Equation (3):

$$MR = \frac{M(t) - M_{eq}}{M_0 - M_{eq}} = \frac{8}{\pi^2}\sum_{n=1}^{\infty}\frac{1}{(2n-1)^2}\exp(-(2n-1)^2\pi^2\frac{D_{eff}t}{4L^2}) \tag{3}$$

Where, D_{eff} is effective diffusivity coefficient (m^2/s), L is effective thickness of slab (m).

Equation (2) takes into account only the first two terms of the solution series, with the assumptions of infinite slab, constant diffusion coefficient and constant initial moisture content equal to M_0.

A variation of the basic equation (Equation (1)) is also reported. Page introduced the homonymous thin-layer drying equation for shelled corn [19]:

$$MR = \exp(-kt^n) \tag{4}$$

Where, k is constant. The equation (4) was modified by Wang and named as Modified Page model (Equation (5)) [20]:

$$MR = A\exp(-kt^n) \tag{5}$$

Where, A and k are constants. Finally, in this work two models (Equation (6) and Equation (7)) based on the Weibull distribution and Attenuation Index equation have been also considered [11]:

$$MR = a - b\exp[-(kt^n)] \tag{6}$$

$$MR = a + b\exp(-t/c) \tag{7}$$

Where *a, b, c, k* are proportionality constants.

Most of the mathematical models used in the studies dealing with the high moisture MSW drying are given in Table 1.

Table 1. Mathematical Models for Drying Curves

Type	model	Expression
Semi-theoretical	Two term exponential	$MR = a\exp(-k_0 t) + b\exp(-k_1 t)$
Semi-empirical	Lewis	$MR = \exp(-kt)$
	Page	$MR = \exp(-kt^n)$
	Modified page	$MR = A\exp(-kt^n)$
empirical	Weibull distribution	$MR = A - B\exp[-(kt^n)]$
	Attenuaion Index	$MR = A + B\exp(-t/C)$

The drying data (drying curves) were analyzed using non-linear regression techniques and the different models were fitted by means of a numerical curve-fitting computer program. The best fitting equation was selected based on the correlation coefficient R^2 (Equation (8)) and the chi-square (γ^2) (Equataion (9)). The lower the value of chi-square γ^2 and the higher the value of the correlation coefficient R^2 (close to 1) the best fitting of the drying data were achieved.

$$R^2 = 1 - \frac{\sum_{i=1}^{N}\left(MR_{pre,i} - MR_{\exp,i}\right)^2}{\sum_{i=1}^{N}\left(\overline{MR_{pre}} - MR_{\exp,i}\right)^2} \tag{8}$$

$$\gamma^2 = \frac{\sum_{i=1}^{N}\left(MR_{pre,i} - MR_{\exp,i}\right)^2}{N-P} \tag{9}$$

Where $MR_{pre,i}$ is the ith predicted moisture ratio, $MR_{exp,i}$ is the ith experimental moisture ratio, N is the number of observations and P is the number of constants in drying model.

3. Results and Discussion

3.1. The Effect of Temperature

Figure 2 shows the effect of temperature on moisture ratio of carrot peel. When the drying temperature increases from 80 to 110℃ and from 110 to 140℃, the interval of the drying curve is to be significantly greater than the other temperature intervals. The interval between the curves decreases as the increasing of temperature. As the temperature level increases constantly, the drying rate varies. At lower temperatures (80-110℃) the drying process of carrot peel is more significantly than higher temperatures (140℃). This is because the higher temperature there is a greater heat transfer driving force (temperature difference) results in the faster drying rate and a shorter drying time. For pomelo peel drying (Figure 3), the change of the drying curve that caused by the constant level of temperature change shows significant difference. The largest interval appears between 105 to 115℃ and the smallest interval is between 115 to 125℃. The interval differences between the carrot peel and pomelo peel is due to the different internal structure of the two samples. The internal cellular structure of the carrot peel is even. There are two layers of pomelo peel with similar thickness. The outer layer of pomelo peel is denser; the inner is soft and sparse, which leads to evaporating process more difficult than carrot peel.

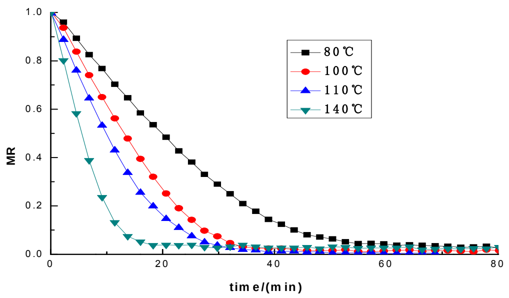

Figure 2. Effect of Temperature on Moisture Ration of Carrot Peel

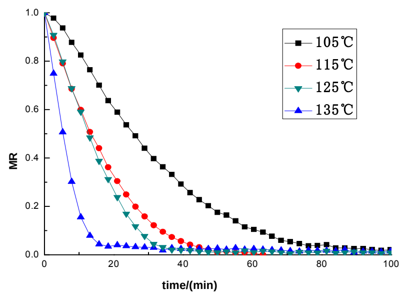

Figure 3. Effect of Temperature on Moisture Ration of Pomelo Peel

Figure 4 and Figure 5 show the effect of temperature on drying rate of carrot peel and pomelo peel respectively. It can be seen from the figures that the whole drying process can be divided into 3 periods: adjustment period, constant rate period and falling rate period. At 80℃, the drying process has a longer period in the constant speed section, and when the temperature is higher to 140℃, constant speed is less obvious than the falling rate section. In the initial stage of the drying process, the internal moisture gradient in the waste changes very rapidly. The drying rate also rises rapidly with the increase of drying temperature until it reaches the maximum drying rate. The internal moisture transfer has been the controlling factors. The surface water evaporates gradually slow down with the increasing temperature, and the drying rate also begins to gradually slow down until the end of the drying process. It indicated that the changes of moisture evaporation in carrot peel and pomelo peel are gradually in depth, and moisture diffusion inside the waste is a non-steady state process. Figure 4 also shows that the moisture value at the maximum rate decreases with increasing temperature. This is because that the temperature difference inside the carrot peel increases with the increasing drying temperature, which is the main driving force for transfer heat and weight. As a result the internal resistance against water evaporation has decreased, and therefore increases the drying depth. This same phenomenon also occurs with the pomelo peel.

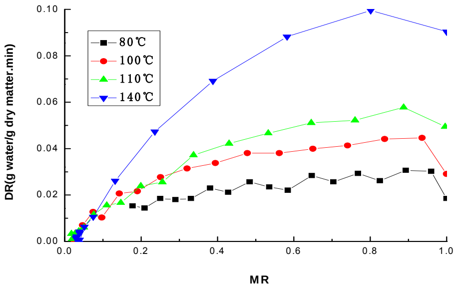

Figure 4. Effect of Temperature on Drying Rate of carrot peel

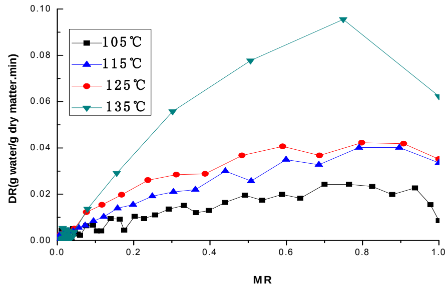

Figure 5. Effect of Temperature on Drying Rate of Pomelo Peel

3.2. Validation of the Proposed Models

Table 2-3 list the fitting results (correlation coefficient and chi-squared) of carrot peel and pomelo peel respectively. It can be seen from tables 2-3 that Modified page model and Weibull distribution have the lower the value of chi-square γ^2 and the higher the correlation coefficient R^2 (close to 1) respectively (with the best fitting model in bold characters). It is evident that the fitting performance follows the general rule of the regression analysis: the more coefficients introduced the more accurate predictions are obtained. Overall, it can be concluded that the best fitting models over the entire test matrix are those based on the Modified page model and Weibull distribution.

Table 2. The Fitting Results of Carrot Peel

Model	Temperature							
	80°C		100°C		110°C		140°C	
	R^2	γ^2	R^2	γ^2	R^2	γ^2	R^2	γ^2
Two term exponential	8.490×10^{-4}	0.9871	7.291×10^{-4}	0.9859	5.909×10^{-4}	0.9936	5.606×10^{-4}	0.9792
Lewis	1.288×10^{-3}	0.9800	1.233×10^{-3}	0.9751	1.300×10^{-3}	0.9843	6.197×10^{-4}	0.9760
Page	3.479×10^{-4}	0.9945	1.479×10^{-4}	0.9970	4.683×10^{-5}	0.9994	3.965×10^{-4}	0.9847
Modified page	**3.508×10^{-4}**	**0.9946**	**1.439×10^{-4}**	**0.9971**	**4.024×10^{-4}**	**0.9995**	**4.015×10^{-4}**	**0.9845**
Weibull distribution	**7.266×10^{-5}**	**0.9989**	**5.477×10^{-5}**	**0.9989**	**3.572×10^{-5}**	**0.9996**	**5.754×10^{-5}**	**0.9979**
Attenuaion Index	8.606×10^{-4}	0.9868	8.606×10^{-4}	0.9868	7.952×10^{-4}	0.9883	3.106×10^{-4}	0.9883

Table 3. The Fitting Results of Carrot Peel

Model	Temperature							
	115°C		125°C		135°C		105°C	
	R^2	γ^2	R^2	γ^2	R^2	γ^2	R^2	γ^2
Two term exponential	6.690×10^{-4}	0.9935	2.904×10^{-4}	0.9974	9.202×10^{-4}	0.9971	3.847×10^{-4}	0.9901
Lewis	2.370×10^{-3}	0.9753	1.426×10^{-3}	0.9852	1.563×10^{-3}	0.9765	6.475×10^{-4}	0.9822
Page	5.051×10^{-5}	0.9995	1.054×10^{-4}	0.9990	1.395×10^{-5}	0.9980	3.749×10^{-4}	0.9900
Modified page	**4.795×10^{-5}**	**0.9995**	**8.898×10^{-5}**	**0.9992**	**1.284×10^{-4}**	**0.9982**	**3.834×10^{-4}**	**0.9900**
Weibull distribution	**3.466×10^{-5}**	**0.9997**	**5.683×10^{-5}**	**0.9995**	**8.856×10^{-5}**	**0.9988**	**6.350×10^{-5}**	**0.9984**
Attenuaion Index	8.233×10^{-4}	0.9918	4.037×10^{-4}	0.9962	0.00116	0.9833	4.326×10^{-4}	0.9887

The values of the Modified Page and Weibull distribution models coefficients (Equation (5) and Equation (6)), were reported in Table 4 and Table 5 respectively.

Table 4. Regression Analysis Coefficients for the Modified Page Model

Model	Temperature 80°C	100°C	110°C	140°C
Modified Page	A=0.992 k=0.0117 n=1.377	A=0.984 k=0.0138 n=1.525	A=0.987 k=0.0308 n=1.361	A=1.005 k=0.0739 n=1.334
Weibull distribution	A=0.0214 B=-0.956 k=0.00821 n=1.496	A=0.0107 B=-0.969 k=0.0123 n=1.574	A=0.00339 B=-0.982 k=0.0300 n=1.374	A=0.0195 B=-0.978 k=0.0639 n=1.428

Table 5. Regression Analysis Coefficients for the Weibull Distribution Model

Model	Temperature			
	105°C	115°C	125°C	135°C
Modified Page	A=1.008 k=0.00837 n=1.364	A=0.982 k=0.0233 n=1.298	A=0.980 k=0.0150 n=1.505	A=1.000 k=0.0792 n=1.320
Weibull distribution	A=0.00795 B=-0.996 k=0.00758 n=1.396	A=-0.0155 B=-1.004 k=0.0266 n=1.243	A=0.00774 B=-0.969 k=0.0138 n=1.540	A=0.0191 B=-0.976 k=0.0698 n=1.407

The quality of models predictions obtained when experimental data were approximated by using the Modified Page and Weibull distribution model for carrot peel and pomelo peel are depicted in Figure 6 and Figure 7 respectively, the predicted data marked with black colour lines and the experimental data with symbols.

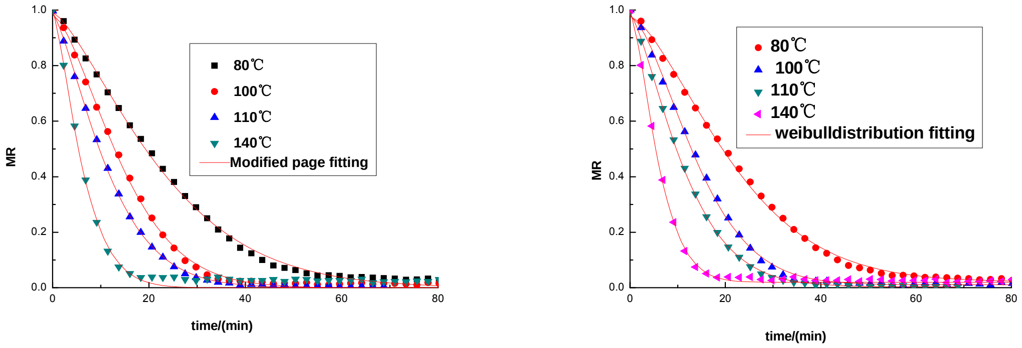

Figure 6. Drying curves (symbols) and approximation (lines) using Modified page model(a) and Weibull distribution model(b) for different temperature values for carrot peel

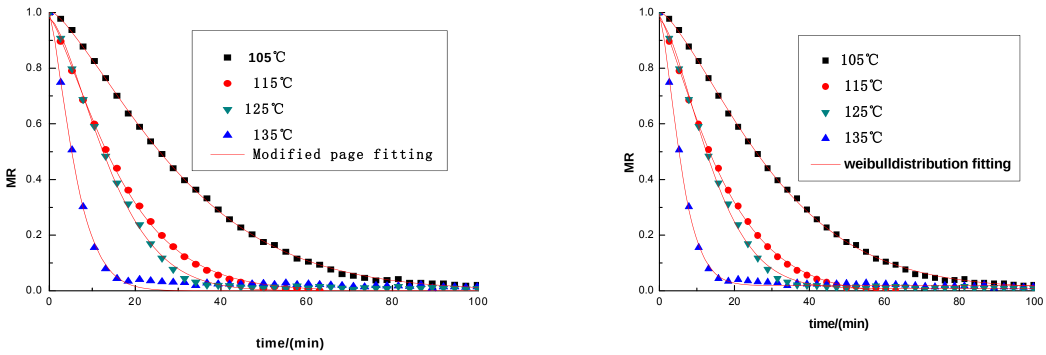

Figure 7. Drying curves (symbols) and approximation (lines) using Modified page model(a) and Weibull distribution model(b) for different temperature values for pomelo peel

The validation of the determined models were established by comparing the experimental data, for each drying curve, with the values predicted by the Modified Page model and the Weibull distribution model the results are plotted in Figure 8. The data points are banded around a 45o straight line, demonstrating the suitability of the models in describing the drying behavior of pomelo peel. As it can be observed, the exponential of Modified Page model (Figure 8(a)) and the Weibull distribution model (Figure 8(b)) predict accurately the experimental curves, which provided a satisfactory estimation of the moisture variation, mainly at lower temperatures.

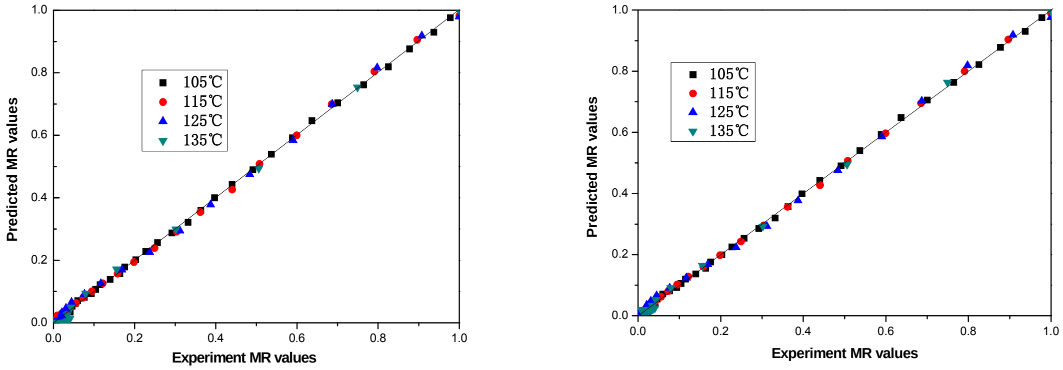

Figure 8. Drying curves (symbols) and approximation (lines) using the Modified Page model(a) and Weibull distribution model (b) for different temperature values for pomelo peel

3.3. Effective Moisture Diffusivity and Activation Energy

In light of the results and the literature surveyed, the Fick diffusion model assumption was suitable to analyze the drying behavior of carrot peel and pomelo peel. Assuming uniform internal moisture distribution, long drying times and negligible external resistance, the analytical solution (Equation (10)) for one-dimensional rectangular coordinates and for overall product moisture is [21]:

$$MR = \frac{8}{\pi^2}\exp(-\pi^2 D_{eff} t / 4L^2) \tag{10}$$

Where L is the thickness of slab (m) for drying from one side, D_{eff} is the effective moisture diffusivity (m^2/s) and t is the drying time (s).

Logarithmic computation for Equation (10), and ln(MR) as a function of time plot. A linear regression analysis was employed to calculate Deff values from the slopes of straight lines. From the logarithmic drying curves, the average D_{eff} values were obtained for each temperature at changing slopes. Table 6 and Table 7 list the effective moisture diffusivity of experimental samples, respectively.

Table 6. Effective Diffusivity of Carrot Peel at Various Temperatures

Temperature/°C	80	100	110	140
D_{eff} / m^2/s	1.49×10^{-9}	2.77×10^{-9}	3.29×10^{-9}	3.57×10^{-9}

Table 7. Effective Diffusivity of Pomelo Peel at Various Temperatures

Temperature/°C	105	115	125	135
D_{eff} / m^2/s	4.79×10^{-9}	9.27×10^{-9}	1.13×10^{-8}	1.25×10^{-8}

Natural logarithms of the calculated diffusivity values was plotted against the inverse of the absolute temperature to find the activation energy using an Arrhenius type relationship (Equation (11)) [22].

$$D_{eff} = D_0 \exp[-E_a/(R_g T)] \tag{11}$$

Where D_0 is Arrhenius factor (m^2/s), E_a is the energy of activation for diffusion (kJ/mol), T is the absolute temperature (K) and R_g is the gas constant (8.314kJ/mol K).

The calculated activation energy is 17.12kJ/mol for carrot peel and 37.48kJ/mol for pomelo peel respectively. Similar activation energy values have been found by S.Simal as 27.0 kJ/mol for kiwi fruit [14], by Chenyunxuan 23.82kJ/mol for potato block and 23.67kJ/mol for cabbage stem [23].

4. Conclusion

Experiments had been carried out for drying of carrot peel and pomelo peel in cubic-type electric furnace, the effect of temperature on drying characteristic, and diffusivity and activation energy were investigated. In the present study several mathematical drying models, available in the literature, were fitted to experimental data obtained when samples were dried in the range of temperatures of 80-140℃.

The analysis, based on non-linear regression techniques, utilizing the estimation of the models' capability to accurately describe the convective drying of high moisture MSW that occurred predominantly in the falling rate period for the entire range of temperature was investigated. The correlation coefficients, for all models were considered and estimated, and the Modified Page and Weibull distribution models demonstrated the best performance in fitting the experimental data. These mathematical modelings of MSW containing high moisture greatly help to optimize operating parameters and improve incineration drying system.

Acknowledgements

This work was supported by National Key Basic Research Program of China (973 Program, 2011CB201501) and Innovation Talent Training Project on Outstanding Youth in Guangdong University, China (LYM09092)

References

[1] Li Jun, Li Xue. The analysis of thermal calculation for air stove drying system. *TELKOMNIKA Indonesian Journal of Electrical Engineering*. 2012; 10(4): 687–692.
[2] Ma Xingguan, Wang Jiao, Xue Xiangxin, et al. Simulation Biomass Effecting On Microbial Fuel Cell Electricity Properties and Substrate Degradation. *TELKOMNIKA Indonesian Journal of Electrical Engineering*. 2013; 11(2): 559−566.
[3] Yang YB, Goh YR, Zakaria R, et al. Mathematical modelling of MSW incineration on a travelling bed. *Waste Management*. 2002; 22: 369~380.
[4] Roberts JS, Kidd DR, Padilla-Zakour O. Drying kinetics of grape seeds. *Journal of Food Engineering*. 2008; 89: 460-465.
[5] Meziane S, Mesbahi N. Determination of moisture diffusivity and activation Energy in thin layer drying of olive pomace. *International Journal of Food Engineering*. 2012; 8(3): 1556-3758.
[6] Chen Deng-yu, Zheng Yan, Zhu X-ifeng. Determination of effective moisture diffusivity and drying kinetics for poplar sawdust by thermogravimetric analysis under isothermal condition. *Bioresource Technology*. 2012; 107: 451–455.
[7] Vega-Gálvez A, Miranda M, Díaz LP, et al. Effective moisture diffusivity determination and mathematical modelling of the drying curves of the olive-waste cake. *Bioresource Technology*. 2010; 101(19): 7265-7270.
[8] Chen C, Wu PC. Thin-layer drying model for rough rice with high moisture content. *Journal of Agricultural Engineering Research*. 2001; 80: 45-52.
[9] Garau MC, Simal S, Femenia A, et al. Drying of orange skin: drying kinetics modeling and functional properties. *Journal of Food Engineering*. 2006; 75: 288-295.
[10] Ruíz DG, Martínez-Monzó J, Fito P, et al. Modelling of dehydration-rehydration of orange slices in combined microwave/air drying. *Innovative Food Science & Emerging Technologies*. 2003; 4: 203-209.
[11] Chen MQ, Chen YX, Jia L. Experimental study on the drying of the high moisture MSW. *Journal of Environmental Sciences*. 2008; 28: 951-955.
[12] Akpinar E, Midilli A, Bicer Y. Single layer drying behaviour of potato slices in a convective cyclone dryer and mathematical modeling. *Energy Conversion and Management.* 2003; 44: 1689-1705.

[13] Akpinar EK. Determination of suitable thin layer drying curve model for some vegetables and fruits. *Journal of Food Engineering*. 2006; 73: 75-84.
[14] Simal S, Femenia A, Garau MC. Use of exponential, Page's and diffusional models to simulate the drying kinetics of kiwi fruit. *Journal of Food Engineering*. 2005; 66: 323-328.
[15] Babalis SJ, Papanicolaou E, Kyriakis N, et al. Evaluation of thin-layer drying models for describing drying kinetics of figs (Ficus carica). *Journal of Food Engineering*. 2006; 75: 205-214.
[16] Vergara F, Amezaga E, Barcenas ME, et al. Analysis of the drying processes of osmotically dehydrated apple using the characteristic curve model. *Drying Technology*. 1997; 15: 949-963.
[17] Lewis W K. The rate of drying of solid materials. *Industrial Engineering Chemistry*. 1921; 13: 427-432.
[18] Sharaf-Eldeen YI, Blaisdell JL, Hamdy MY. A model for ear corn drying. *Transactions of the ASAE*. 1980; 23: 1261-1265.
[19] Page GE. Factors influencing the maximum rates of air drying shelled corn in thin layers. PhD Thesis. West Lafayette: Purdue University. 1949.
[20] Babalis SJ, Papanicolaou E, Kyriakis N, et al. Evaluation of thin-layer drying models for describing drying kinetics of figs(Ficuscarica). *Journal of Food Engineering*. 2006; 75: 205-214.
[21] Senadeera W, Bhandari BR, Young G, et al. Influence of shapes of selected vegetable materials on drying kinetics during fluidized bed drying. *Journal of Food Engineering*. 2003; 58: 277-283.
[22] Jin Park K, Vohnikova Z, Pedro Reis Brod F. Evaluation of drying parameters and desorption isotherms of garden mint leaves (Mentha crispa L). *Journal of Food Engineering*. 2002; 51: 193-199.
[23] CHEN YX. Experimental study on the drying of typical MSW on incinerator-like conditions. Master Thesis. Beijing: Beijing Jiaotong University. 2007.